

IMECE2010-37-) +

## ENERGY PAYBACK OPTIMIZATION OF THERMOELECTRIC POWER GENERATOR SYSTEMS

**Kazuaki Yazawa**

Dept. of Electrical Engineering,  
University of California Santa Cruz  
Santa Cruz, CA 95064 USA

**Ali Shakouri**

Dept. of Electrical Engineering,  
University of California Santa Cruz  
Santa Cruz, CA 95064 USA

### ABSTRACT

An analytic model for optimizing thermoelectric power generation system is developed and utilized for parametric studies. This model takes into account the external thermal resistances with hot and cold reservoirs. In addition, the spreading thermal resistance in the module substrates is considered to find the impact of designing small fraction of thermo elements per unit area. Previous studies are expanded by a full optimization of the electrical and thermal circuits. The optimum condition satisfies both electrical load resistance match with the internal resistance and the thermal resistance match with the heat source and the heat sink.

Thermoelectric element aspect ratio and fill factor are found to be key parameters to optimize. The optimum leg length and the maximum output power are determined by a simple formula. The output power density per mass of the thermoelectric material has a peak when thermo elements cover a fractional area of ~1%. The role of the substrate heat spreading for thermoelectric power generation is equally significant as thermoelement.

For a given heat source, the co-optimization of the heat sink and the thermoelectric module should be performed. Active cooling and the design of the heat sink are customized to find the energy payback for the power generation system. The model includes both the air cooled heat sinks and the water cooled micro channels. We find that one can reduce the mass of thermoelement to around 3~10% of that in commercial modules for the same output power, as long as the module and elements are designed properly. Also one notes that higher heat flux sources have significantly larger energy payback and reduced cost per output power.

### NOMENCLATURE

A: Area (TE substrate or fin) [m<sup>2</sup>]  
C: Thermal resistance ratio [(W/K)/(K/W)]  
C<sub>p</sub>: Specific heat [W/mK]  
D: Width of heat sink or channel [m]  
d: Leg length [m]  
F: Fill factor (fraction of element)  
I: Current [A]  
L: Length of fluid passage of heat sink or channel [m]  
m: Electric resistance ratio [ohm/ohm]  
q: Heat flow [W/m<sup>2</sup>]  
R: Electrical resistance of element [ohm]  
S: Seebeck coefficient [V/K]  
T: Temperature [K]  
U: Heat transfer coefficient [W/m<sup>2</sup>K]  
u: Fluid flow speed [m/s]  
w: Power per unit area [W/m<sup>2</sup>]  
Z: Figure of merit [1/K]

### GREEK SYMBOLS

β: Thermal conductivity [W/mK]  
δ: fin spacing [m]  
φ: Spreading angle [deg]  
η: Efficiency  
λ: Dimension thickness of substrate  
ρ: Density [kg/m<sup>3</sup>]  
σ: Electrical conductivity [S]  
ψ: Thermal resistance [K/W]

### SUBSCRIPTS

a: ambient  
BASE: heat sink foot print

c: cold side  
 fin: fins or channel walls  
 f: fluid  
 h: hot side  
 HS: heat sink  
 pp: fluid pumping  
 s: source for T:temperature, substrate for A: area

## 1. INTRODUCTION

Energy technologies are getting significant attention for sustainability. There are many ways to generate power from a heat source. Here, we focus on solid state thermoelectric energy conversion due to its simple mechanical structure, scalability, and the potential use in distributed power generation and waste heat recovery. Thermoelectrics, due to their moderate energy conversion efficiency, have had limited applications such as in wrist watch [1], vehicle exhaust [2], extraterrestrial ship [3] and autonomous sensors on the body [4]. In rare case, it is also observed for electronics application [5].

Since there is no general model commonly accepted for the whole thermoelectric power generation system, most of above work required significant amount of engineering parametric analysis. However, it is hard to separate requirements for specific application and the general thermoelectric system design guidelines since so many parameters are involved.

In this study, an analytic model for optimizing thermoelectric power generation system is developed and utilized for parametric analysis. The model takes into account the external thermal resistances with the hot and cold reservoirs. In addition, the spreading thermal resistance in the thermoelectric module's substrates is considered to find the impact of having a small fraction of thermo elements per unit area. This influences significantly the amount of power generated per unit mass of the material. Previous work is expanded by a full optimization of the electrical and thermal circuits.

In the previous studies, most of the attention was focused on the thermoelectric element. However, heat flow is a significant factor affecting the output power so the full thermal system modeling is quite important. Similar approach is found in the work of Fukutani et al. optimizing thermoelectric refrigerators for integrated circuit cooling applications [6]. In the case of power generation, there are a few important studies which consider both the thermo elements and the external thermal resistances. Mayer et al. pointed out, that there is an optimum thickness of the TE element when it is thermally matched to the cold side heat sink. This work ignores Peltier and Joule effects in the heat transfer, as well as the hot side heat sink thermal resistance [7]. Stevens modeled a thermoelectric system with two external thermal resistances. The maximum output power was achieved when internal thermal resistance matched the sum of external thermal resistances. The model is limited to small temperature gradients and electrical impedance matching is not in consideration [8]. Snyder discussed thermal resistance match in a thermal circuit and obtained maximum power formula as a function of conversion

efficiency [9]. Also, Snyder considered the match of the electrical load and the maximum efficiency condition. It concludes that maximum efficiency configuration for system design leads to slightly shorter leg lengths [10].

In this paper, contributions of the thermoelectric element length, external load resistance, external thermal resistances and the fill factor are considered. Not only power output per unit area but also material mass usages are investigated. To understand energy payback, power consumption of the cooling solution is modeled for air convection heat sink with fan and water cooled micro channels with pump. The model is designed to be scalable as a function of the heat source power density and the fluid passage is optimized to obtain the best performance for a given pumping power. The impact of the thermoelectric figure-of-merit, material costs for TE elements, substrates and the heat sink are studied on the amount of energy generated per unit mass.

## 2. FULL OPTIMIZATION OF ELECTRO THERMAL SYSTEM

We have developed a generic model of the thermoelectric module taking into account external finite thermal resistances with hot and cold reservoirs. The system is defined as a thermal network shown in Fig 1 in analogy of electric circuit. Resistance in the figure shows thermal resistance, current represents heat flow and electric potential is translated to temperature, respectively. The geometry of the thermoelement is optimized considering spreading or constriction thermal resistances on both sides. Area fraction ratio which a thermoelement occupies per unit substrate area is defined as F: fill factor. If the fill factor is equal to 1, thermal resistances  $\psi_{hs}$  and  $\psi_{cs}$  are just the thermal resistance of the substrate. Electric potential generated in the thermoelement induces electric current flow when an external load (that is for extracting electricity) is connected to the electrodes. In the thermal network, generated electrical current yields heat transport as known as Peltier effect and produces Joule heating in the element. Both are described as current (heat) sources at the terminals while the element is considered as a thermal resistor.

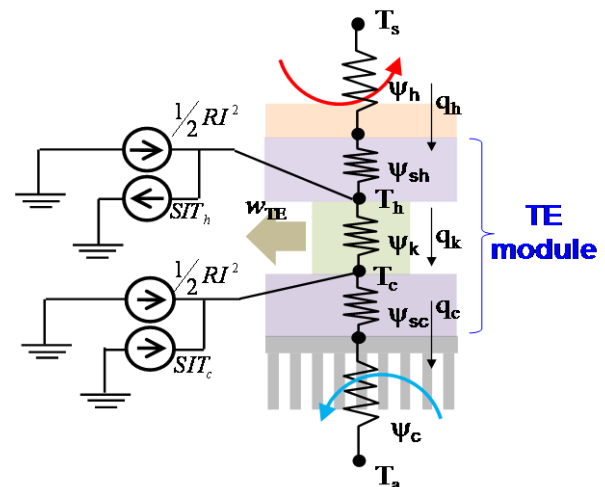


Figure 1. Equivalent thermal circuit of the TE module with heat source and heat sink

To study the impact of the factors clearly in this first order model, contact interface resistances in electrical and thermal regimes as well as the parasitic heat losses by radiative heat transfer is not included.

Thermal or electrical current distribution inside the element is not considered in this model. Heat flow balance at the two nodes  $T_h$  and  $T_a$  can be expressed as the following:

$$\frac{1}{\psi_k}(T_h - T_c) = \frac{1}{\psi_h + \psi_{sh}}(T_s - T_h) - S I T_h + \frac{I^2 R}{2} \quad (1)$$

$$\frac{1}{\psi_c + \psi_{sc}}(T_c - T_a) = \frac{1}{\psi_k}(T_h - T_c) + S I T_c + \frac{I^2 R}{2} \quad (2)$$

where,

$$\psi_k = \frac{d}{\beta F A}, \quad R = \frac{d}{\sigma F A} \quad (3)$$

One can rewrite Eq (1) and Eq (2) by introducing  $m$ : the external load electrical resistance relative to the internal resistance,

$$\frac{1}{\psi_h + \psi_{sh}}(T_s - T_h) = \frac{1}{\psi_k}(T_h - T_c) + \frac{\beta F A Z}{(1+m)^2 2d} ((2m+1)T_h + T_c)(T_h - T_c) \quad (4)$$

$$\frac{1}{\psi_c + \psi_{sc}}(T_c - T_a) = \frac{1}{\psi_k}(T_h - T_c) + \frac{\beta F A Z}{(1+m)^2 2d} (T_h + (2m+1)T_c)(T_h - T_c) \quad (5)$$

Temperature difference across the thermoelement relative to the system temperature difference can be found as,

$$\frac{(T_h - T_c)}{(T_s - T_a)} = \frac{\psi_k}{\psi_k + \frac{q_h}{q_k} \Psi_h + \frac{q_c}{q_k} \Psi_c} \quad (6)$$

Due to the complexity, one can assume  $\Psi_h = \Psi_c$  in the first analysis. Introducing  $T_s$  and  $T_a$ ,  $w$ : power output per unit area [ $W/m^2$ ] is written as Eq (7).

$$w = \frac{mZ}{A(1+m)^2} \frac{d\beta F A}{\left( d + \beta F A \left( 1 + \frac{Z\bar{T}}{(1+m)} \right) \sum \Psi \right)^2} (T_s - T_a)^2 \quad (7)$$

where,

$$\sum \Psi = \Psi_h + \Psi_c = (\psi_h + \psi_{sh}) + (\psi_c + \psi_{sc}) \quad (8)$$

In this formula,  $m$  and  $d$ : leg length are parameters which should be optimize. If  $m$  is assumed to be constant.  $d_{opt}$  can be found when the differential of Eq (7) is set to zero,  $\partial d / \partial w = 0$ . Thus,

$$d_{opt} = \beta F A \sum \Psi \left( 1 + \frac{Z\bar{T}}{(1+m)} \right) \quad (9)$$

Similarly, if  $d$  is assumed as constant,  $m_{opt}$  can be found

when  $\partial m / \partial w = 0$ . Then:

$$m_{opt} = \sqrt{1 + Z\bar{T}} \quad (10)$$

$$\psi_k = C \sum \Psi \quad (11)$$

Numerical investigation was carried out to show that the two solutions hit a single peak maximizing the power output. Interestingly,  $m$  and  $C$  both match to the same value at the optimum. The example case when  $Z\bar{T}=1$  is shown in Fig 2.

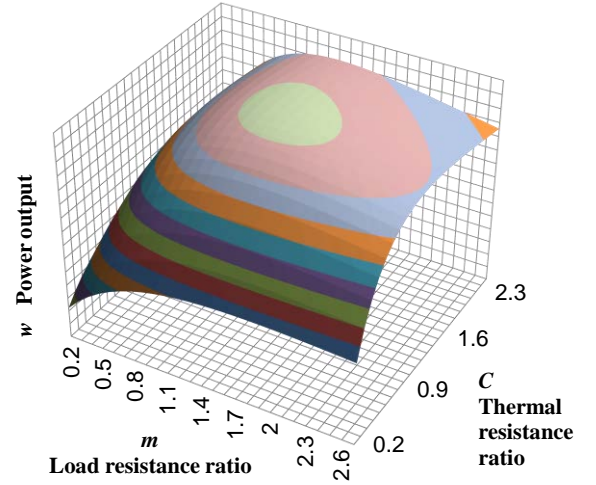


Figure 2. Full optimization of the power output.  $m$ : electrical resistance ratio and  $C$ : leg thermal resistance ratio for  $F=1$ ,  $Z\bar{T}=1$ , peak is found at  $m=1.414$  and  $C=1.414$

Finally, the maximum power density is found as,

$$w = \frac{Z}{4(1+m)^2} \frac{1}{A \sum \Psi} (T_s - T_a)^2 \quad (12)$$

when

$$d = m\beta F A \sum \Psi \quad \text{and} \quad m = \sqrt{1 + Z\bar{T}} \quad (13)$$

One can verify that in other extreme cases such as  $\Psi_h \rightarrow 0$  or  $\Psi_c \rightarrow 0$ , the same optimum is found. Thus, this solution is a general formula.

### 3. SPREADING THERMAL RESISTANCE

Typically, thermoelement legs do not occupy the whole foot print of the substrate. Since small fraction of fill factor reduces the heat flow cross section area, spreading/constriction thermal resistance should be taken into account. The thermal resistance is not just a linear function of the fractional area. Fig. 3 shows the simplified model. Leg cross section shape is considered as square and the cross section area of leg is defined by  $a^2$  here.

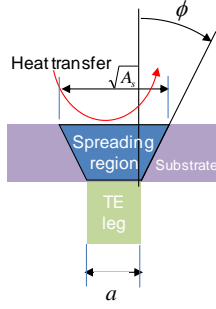


Figure 3. Thermal spreading by fraction of fill area

In the electronics industry, it is popular to use Song et.al. model [11]. However, despite the good engineering accuracy, the boundaries of the heat spreading region are not clear. In this study, instead, we utilized Vermeersch et al. model which has a clear boundary of spreading limit up to 46.45 deg angle for smaller fraction [12]. One should note that this fixed angle model introduces some error due to the assumption of uniform temperature at heat transfer surface. However as a first order analysis, in order to optimize the output power and efficiency, this should be sufficient. The spreading thermal resistance is written as,

$$\psi_{sh} = \psi_{sc} = \frac{\lambda}{\beta_s a (1 + 2\lambda t a \pi \phi)} \quad (14)$$

where,

$$\begin{cases} \phi = 5.86 \ln(\lambda) + 40.4 & 0.0011 < \lambda \leq 1 \\ \phi = 46.45 - 6.048 \lambda^{-0.969} & \lambda \geq 1 \end{cases} \quad (15)$$

and,

$$\lambda = d_s / a \quad (16)$$

Where,  $a$  is width of leg,  $\phi$  is spreading angle. As determined, substrate thickness  $d_s$  and thermal conductivity  $\beta_s$  play a significant role in spreading. For small fractional coverage, the area outside of the spreading region does not influence the heat flow in the thermoelectric elements. Thus, it is natural to consider packing of the elements until the boundaries of the spreading regions touch each other. The limit condition can be expressed as,

$$F = \left(1 - \frac{2d_s t a \pi \phi}{a}\right)^2 \quad (17)$$

#### 4. POWER OUTPUT WITH FRACTIONAL COVERAGE OF TE ELEMENT

Taking into account spreading resistance, sum of external thermal resistance in Eq (12) and Eq (13) becomes Eq (18).

$$\sum \Psi = \Psi_h + \Psi_c + \frac{2\lambda}{\beta_s a (1 + 2\lambda t a \pi \phi)} \quad (18)$$

Output power density as a function of fractional coverage (fill factor) is shown in Figure 4.

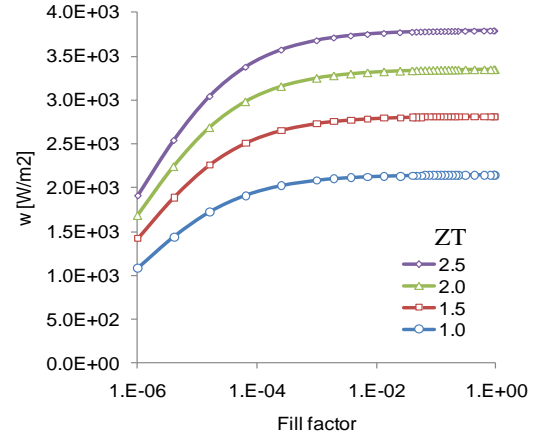


Figure 4. Power density versus fill factor for different ZT's when  $T_s=600$  [K],  $T_a=300$  [K],  $\beta_s=140$  [W/mK],  $d_s=0.2e-3$  [m],  $U_h, U_c=500$  [W/m<sup>2</sup>K]

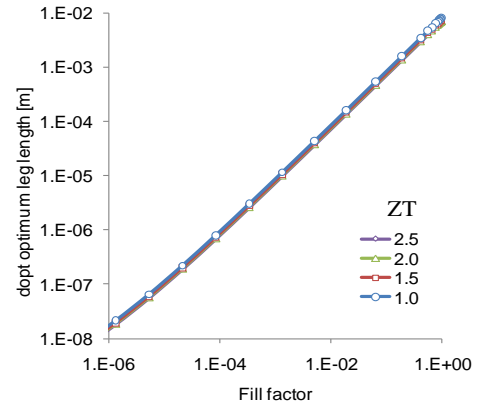


Figure 5. Optimum leg length versus fill factor for different ZT's at the same condition as Fig 5.

When the fill factor is more than 1%, the output power almost does not change. However, the optimum leg length keeps shrinking as long as the fill factor is reduced. (see Fig. 5) This fact is quite beneficial to maximize power per unit mass and indicate the advantage of thermoelement with small fill factor 1%-10%. This suggests that one can essentially reduce thermoelement material approximately down by 1/10,000 (product of 1/100 fill area and 1/100 leg length) with very small performance degradation. On the other hand, when thermo elements cover a small fraction of the surface, the module mass will be dominated by the substrate. In addition thermal spreading resistance at small fractional coverage depends on the thermal conductivity and the thickness of the substrate. Fig. 6 shows output power and Fig. 7 shows power per unit mass of the TE module as a function of the fill factor for different substrate thicknesses. There is an optimum fill factor 0.3-3% which is substrate thickness dependent.

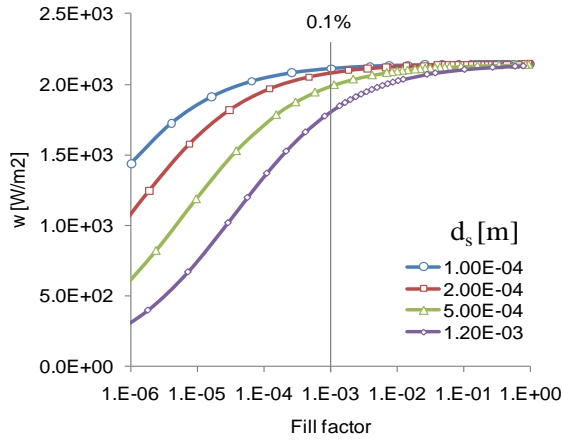


Figure 6. Output power density versus fill factor for different  $d_s$ : substrate thickness for optimum design at  $ZT=1$ ,  $T_s=600$  [K],  $T_a=300$  [K],  $\beta_s=140$  [W/mK],  $U_h, U_c=500$  [W/m<sup>2</sup>K],  $\rho_{TE}=9.78$  [kg/m<sup>2</sup>],  $\rho_{sub}=3.26$  [kg/m<sup>2</sup>]

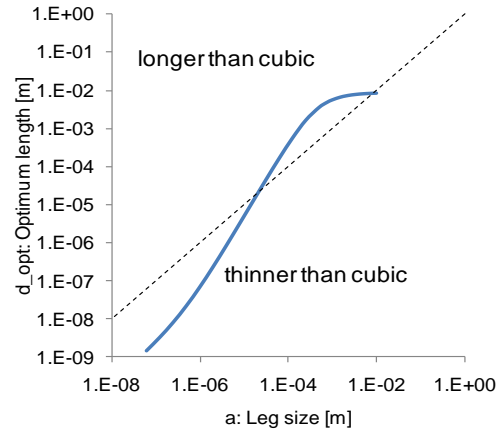


Figure 8. Aspect ratio of the thermoelectric leg optimized by changing fill factor at  $ZT=1$ ,  $T_s=600$  [K],  $T_a=300$  [K],  $\beta_s=140$  [W/mK],  $d_s=0.2e-3$  [m],  $U_h, U_c=500$  [W/m<sup>2</sup>K]

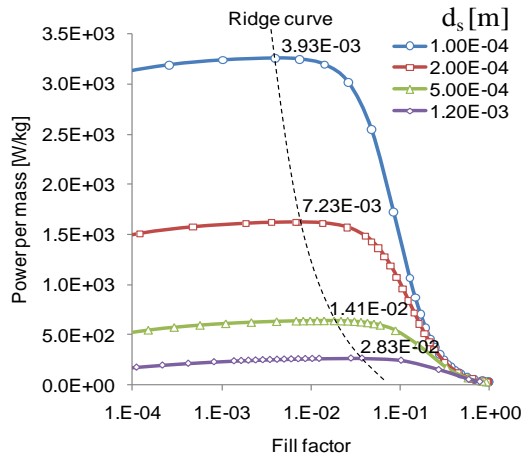


Figure 7. Power output per unit mass versus fill factor for different substrate thicknesses  $d_s$ .

## 5. ASPECT RATIO AND ZT IMPACT

It is interesting to note that the leg aspect ratio, length ( $d$ ) per cross-section diameter ( $a$ ), is not constant as we optimize the thermoelectric module. The details are described in Fig. 8. This non-linear dependence is due to the impact of the thermal spreading resistance. In practical fractional coverage areas  $F > 0.01$ , the optimum aspect ratio can be as much as 10 times larger compared to the simple cubic relationship. In this case, the spreading contribution is small so that the element shape can be longer than cubic. In contrast, for small fractions spreading thermal resistance dominates so that the shape need to be shorter (thinner) than the one predicted by the cubic relation. The trend is shown in Fig. 8. The dashed line in the figure indicates the cubic shape. From the assembly and manufacturing view point of the thermoelectric module, it could be beneficial to reduce the leg length to the range of thinfilm. The small fractional area (e.g. 1%) of thermoelements can be deposited directly on to the substrate with using an appropriately designed mask and therefore nothing is wasted.

Fig. 9 shows the impact of the thermoelectric figure-of-merit on the output power per unit mass. Two cases are considered: changing either thermal conductivity or power factor (Seebeck coefficient square times electrical conductivity). It can be seen that there is no significant difference between the two cases at extremely high ( $F \sim 1$ ) or very low ( $F < 0.01$ ) fractional coverage, but in the middle, improvement of ZT by reducing thermal conductivity is more effective. This is due to the smaller optimum thickness of the TE element matched to the external thermal resistances and the reduced use of the TE material for a given power output.

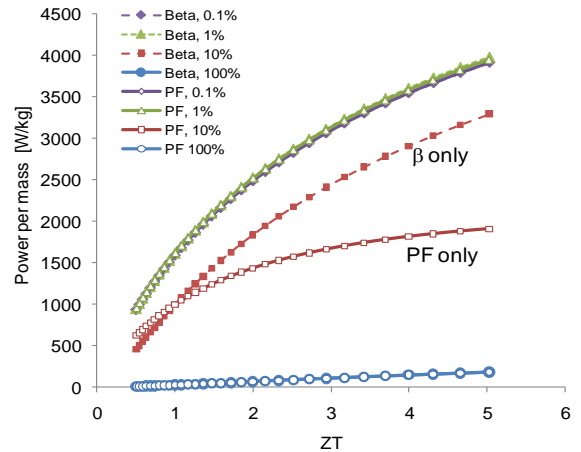


Figure 9. Power per mass by ZT

## 6. COST PERFORMANCE

Once the material cost per weight is given, the cost of the thermoelectric power generation can be easily calculated using the previous power per mass model. There will be always additional cost due to the module fabrication and packaging but at least we can study the impact of the thermoelectric material properties and its cost. As the example, let's assume 500 [\$/kg] for thermoelement (e.g. Bismuth Telluride) and vary it between 100~1000 [\$/kg]. This probably covers most of the cases while

BiTe or PbTe are used. As for the substrate, Aluminum Nitride is considered since it is quite important to have the better thermal conductive material and the cost range of 20~180 [\$/kg] is used. Fig. 10 shows the impact of the TE element fraction coverage on the power generation performance. When  $F > 10\%$ , the price of the TE material dominates the cost performance. In contrast, when  $F < 1\%$ , the price of the substrate dominates the cost performance. For comparison today's photovoltaic cells cost approximately 200 [\$/m<sup>2</sup>] in market based on Purvis [13].

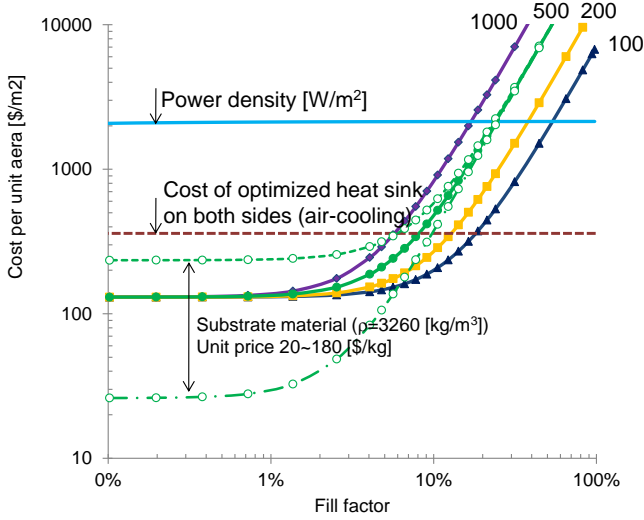


Figure 10. Cost performance of thermoelectric power generation versus the fill factor. Different prices for the TE material and the substrate are assumed.

## 7. HEAT SINK OPTIMIZATION

There is a significant amount of work on heat sink optimization as described e.g. in [14] [15] [16]. In this study, the model of Yazawa et al. [17] is used, but slightly modified in order to do a systematic calculation of the energy payback. We assume a heat sink where the fluid path is made of parallel channels as shown in Fig. 11. This structure corresponds to both air convection cooling and water cooling. The water cooled micro channels are typically designed taking the wall thickness to be constant ( $b$ ) and varying the channel width (fin gap,  $\delta$ ). However, in this study, the mass of the heat sink is important. Thus the wall thickness is assumed to be at its minimum manufacturable value.

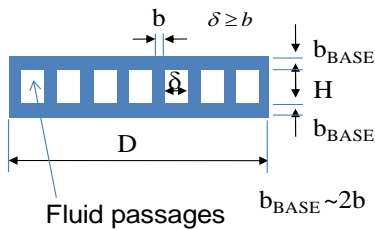


Figure 11. Heat sink model

In this session, we will optimize the channel design for a

given thermal resistance and pumping power in order to minimize its mass. From the discussion in Ref. [17], the optimum condition can be found when the convection from the fin surface matches to that of the temperature sensitive fluid flow. This is a kind of impedance match for heat flow from the fin to the fluid reservoir. The impedance matched condition is described as,

$$U_{BASE} A_{BASE} = 1 / \left( \frac{1}{2\dot{m}C_p} + \frac{1}{U_{fin} A_{fin}} \right) \quad (19)$$

where,

$$A_{fin} = 2N(H + \delta)L \quad \text{and} \quad \dot{m} = \rho N \delta H u \quad (20)$$

From the heat transfer match,  $u$ : flow velocity is found as:

$$u = \frac{N_u \beta_f}{2\rho C_p} \left( \frac{H + \delta}{H\delta} \right)^2 L \quad (21)$$

With considering hydraulic diameter  $D_h$  as

$$D_h = \frac{2H\delta}{(H + \delta)} \quad (22)$$

By combining with the Eq (19),  $U_{BASE}$ : heat transfer coefficient at foot print is found as:

$$U_{BASE} = \frac{N_u \beta_f (H + \delta)^2}{2H\delta(b + \delta)} \quad (23)$$

This equation can be solved in order to determine the optimum  $\delta$  channel spacing.

$$\delta = H \frac{(bx - 1) - \sqrt{(1 - bx)^2 - (1 - 2Hx)}}{(1 - 2Hx)} \quad (24)$$

where,

$$x = \frac{U_{BASE} f}{N_u \beta_f} \quad (25)$$

In above relation,  $Nu$  is the Nusselt number, which is dimensionless heat transfer coefficient and determined by aspect ratio  $\delta/H$  as shown in Eq (26). Here we followed the data of Kays and London [18]. In this study, constant wall temperature and fully developed flow for entire channel are assumed.

$$Nu = 4.52(1 - \delta/H)^{3.78} + 2.98 \quad (26)$$

Pumping power required for this configuration is determined by:

$$w_{pp} = \frac{Nu\delta H\Delta P_{ch}}{A_s} \quad (27)$$

Volume flow rate is found straight forward by the product of velocity and cross section area. Other component is pressure loss throughout the channel flow  $\Delta P_{ch}$  which is given by:

$$\Delta P_{ch} = \frac{K\rho}{2}u^2 + \frac{48\mu L}{D_h^2}u \quad (28)$$

The previous model is valid when the fluid flow regime is laminar. Since the channel wall thickness is small compare to the channel spacing, the first term of Eq (28) can be neglected and the relation to velocity becomes linear. Substituting simplified Eq (28) and Eq (21) into Eq (27), the pumping power as a function of channel spacing is found as:

$$w_{pp} = 3\mu \left( \frac{N_u \beta_f}{\rho C_p} \right)^2 \frac{(H + \delta)^6}{(b + \delta)(H\delta)^5} L^2 \quad (29)$$

Finally, the optimum channel spacing  $\delta$  is found by Eq (24) and the required pumping power is determined by Eq (29).

## 8. ENERGY PAYBACK

Using the formalism in the previous section, the co-optimization of the thermoelectric generator and the heat sink can be performed for various heat sources. The pumping power needed for the convection heat sink will be subtracted from the generated power in order to calculate the energy payback (net output power).

The energy payback as a function of hot side heat flux is plotted in Fig. 12. The analysis contains two different cooling solutions. At low heat fluxes, air convection cooling using blower fan is used. As heat flux increases, fin spacing needs to be decreased in order to extend the convective surface. Simultaneously, the air flow rate must increase to be able to pump more heat. Tighter fins and higher air velocity both require larger pumping power so that the pumping curve increases very steeply as a function of the heat flux. At some point, fan power, which is real electricity not the fluid dynamic power, overtakes the TE power output and payback goes to zero. This happens at around  $1e+5$  [W/m<sup>2</sup>] heat flux in this example. One can design the water cooling channels for higher heat flux. At the same time one needs to consider the cost of the solution. Cost payback is shown Fig. 13. It can be seen that the energy payback becomes greater as heat flux increases. Even water cooling with sophisticated micro channel technology reaches a limit beyond which the pumping power requirement is too high. This depends on the fractional area coverage of the thermo elements. In the best case, the maximum heat flux is around 50MW/m<sup>2</sup>.

Characteristics of thermoelectric power generation can be compared with solar cells. Power density of planar solar cells is limited by the source density (solar irradiation) which is approximately 750 W/m<sup>2</sup> maximum on the incident angle on the ground (as passed through the earth's atmosphere). One can

see that the benefit of using thermoelectrics is largest for higher heat flux sources.

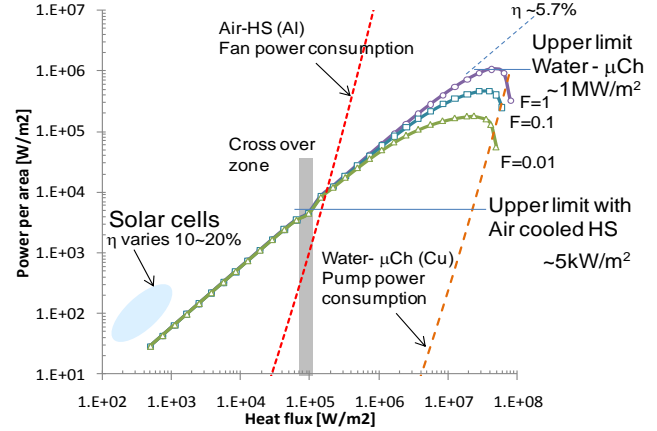


Figure 12. Energy pay back (net output) [W/m<sup>2</sup>] for various heat fluxes:  $ZT=1$ ,  $\beta = 1.5$  [W/mK],  $T_s=600$ K,  $T_a=300$ K, air cooling fan efficiency 30%, water cooling pump efficiency 60%

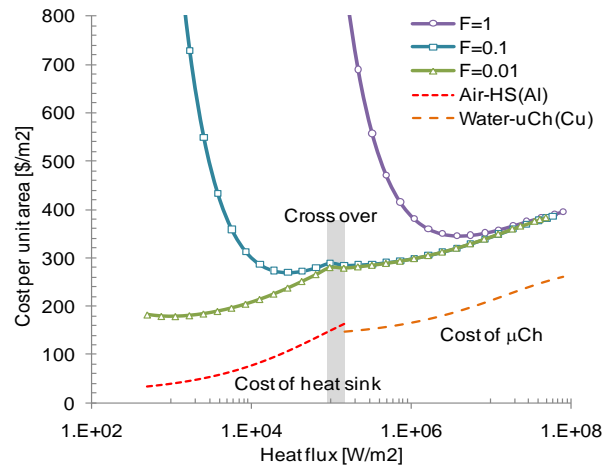


Figure 13. Material cost per unit area of TE power generation system:  $ZT=1$ ,  $b = 1.5$  [W/mK],  $T_s=600$ K,  $T_a=300$ K, Fan efficiency 30%, TE \$30/kg, Substrate-AlN: \$100/kg, Aluminum heat sink: \$1.5/kg, copper microchannel: \$7.3/kg

## 9. CONCLUSIONS

A general formalism is developed for thermoelectric power generation system. The optimum design for the thermoelectric module and the heat sink are identified which can maximize the output power per unit area and the power per unit mass. The optimum design corresponds to the well known electrical impedance match with the internal resistance as well as the thermal resistance match with the sum of the external thermal resistances. Beautiful piece of determining the circumstance of maximum power output in compare to the ordinal circuit is that both resistances match at the same ratio involves the square root of  $1+ZT$ . Thermal conductivity of the thermoelectric material influences the optimum leg length. Aspect ratio is determined by the optimum leg length and the fraction area coverage of the TE elements. Output power density per material mass is found to have a peak around 1% fractional

coverage. One can reduce the mass of thermoelement to around 3~10% of typically available in market for the same output power, as long as the module and elements are optimally designed. The role of module substrate (heat spreader) for thermoelectric power generation is equally significant as the thermo elements. When the cost of the thermoelectric material cannot be neglected, improving ZT by reducing thermal conductivity can have a higher impact in increasing the amount of power per unit mass than the same ZT achieved by increasing the power factor. This is due to the impact of the optimum heat sink thermal resistance.

The model of heat sink performance and pumping power is customized to find the energy payback for the power generation system. Both the air cooled and the water cooled micro channel heat sinks are studied. Also one can note that higher heat flux sources can have lower cost for thermoelectric power generation system.

As a first order analysis, in this work we only considered the mass and the cost of the thermoelectric material and the TE module substrates. In the future, this preliminary optimization will be expanded to take into account the manufacturing and packaging cost as well as the role of non-ideal electrical and thermal resistances. In practical systems, one also has to optimize the mechanical stresses in the module under temperature cycling and this is a key parameter to optimize as a function of the fractional area coverage which influences the optimum TE element leg length. The impact of the factors in this first order model such as contact interface resistances in electrical and thermal regimes as well as the parasitic heat losses by radiative heat transfer will be considered in future work.

## ACKNOWLEDGEMENTS

This work was supported by Center for Energy Efficient Materials funded by the Office of Basic Energy Sciences of the US Department of Energy.

## REFERENCES

- [1] Kishi, M., Nemoto, H., Hamao, T., Yamamoto, M., Sudou, S., Mandai, M. and Yamamoto, S., 'Micro- thermoelectric modules and their application to wristwatches as an energy source', Proceedings of 18th Int. Conf. Thermoelectrics, pp.301-307, (1999)
- [2] Hendricks, T.J., Lustbader, J.A., 'Advanced thermoelectric power system investigations for light-duty and heavy duty applications', 21st International Conference on Thermoelectronics, pp381-394, (2002)
- [3] Bass, J.C. and Allen, D.T., 'Milliwatt Radioisotope Power Supply for Space Applications', Proceedings of 18th International Conference on Thermoelectrics, pp 521-524, (1999)
- [4] Leonov, V., Fiorini, P. Torfs, T., Vullers, R. and Van Hoof, C., 'Thermal matching of a thermoelectric energy harvester with the environment and its application in wearable self-powered wireless medical sensors', Proceedings of 15th Int. Workshop on Thermal investigations of ICs and Systems - Thermic. 2009. pp.95-100, (2009)
- [5] Yazawa, K., Solbrekken, G and Bar-Cohen, A., 'Thermoelectric-Powered Convective Cooling of Microprocessors', IEEE Transaction on Advanced Packaging, Vol. 28, No.2, pp 231-239, (2005)
- [6] Fukutani, K. and Shakouri, A., 'Design of bulk thermoelectric modules for integrated circuit thermal management', IEEE Transactions on Components and Packaging Technologies, vol.29, no.4, pp. 750-757, (2006)
- [7] Mayer, P.M., and Ram, R.J., 'Optimization of Heat Sink-Limited Thermoelectric Generators', Nanoscale and Microscale Thermophysical Engineering, 10: 143-155, (2006)
- [8] Stevens, J. W., 'Optimum design of small DT thermoelectric generation systems', Energy Conversion and Management 42, pp 709-720, (2001)
- [9] Snyder, G J., '11.6 Matched Thermal Resistance, Chap. 11 Thermoelectric Energy Harvesting', Energy Harvesting Technologies, Ed. Shashank Priya and Daniel J. Inman, Springer, pp 330-331, (2009)
- [10] Snyder, G J., '9.6.4 Maximum Power Density/ Matched load, Chap. 9 Thermoelectric Power Generation: Efficiency and Compatibility', Thermoelectrics Handbook Macro to Nano, Ed. D. M. Rowe, Taylor & Francis, pp 9-22 - 9-24, (2006)
- [11] Song, S., Lee, S., and Au, V., 'Closed-Form Equation for Thermal Constriction/Spreading Resistances with Variable Resistance Boundary Condition', Proc. of IEPS 1994 International Electronics Packaging Conference, pp 111-121, (1994)
- [12] Vermeersch, B., and De Mey, G., 'A Fixed-Angle Dynamic Heat Spreading Model for (An)Isotropic Rear-Cooled Substrates', ASME Journal of Heat Transfer Volume 130, Issue 12, 121301, (2008)
- [13] Purvis, G., 'Material, price and power: Expect exciting developments from solar components' suppliers in the coming months and years', Refocus Vol. 8, Issue 1, January-February 2007, pp 42-44, 46-47, (2007)
- [14] Murakami, Y. and Mikic, B.B., "Parametric Optimization of Multichanneled Heat Sinks for VLSI Chip Cooling", IEEE Transaction on Components and Packaging Technologies, Vol. 24, No. 1, pp. 2-9, IEEE (2001)
- [15] Teertstra P., Culham, J.R and Jovanovich, M.M., "Analytic Modeling of Forced Convection in Slotted Plate Fin Heat Sinks", Proceedings of 1999 ASME International Mechanical Engineering Congress and Exposition, HTD-Vol. 364-1, Vol.1, pp. 3-11, ASME (1999)
- [16] Iyengar, M. and Bar-Cohen, A., "Least-Energy Optimization of Air-Cooled Heat Sinks for Sustainable Development", IEEE CPT Transactions, Vol. 26, No.1, pp.16-25, IEEE (2003)
- [17] Yazawa K., Solbrekken, G.L. and Bar-Cohen, A., "Thermofluid Design of Energy Efficient and Compact Heat", Proceedings of 2003 International Electronic Packaging Technical Conference and Exhibition, IPACK2003-35242, ASME (2003)
- [18] Kays and London, 'Fig. 6-3 Nusselt numbers for laminar flow in rectangular tubes with fully developed velocity and temperature problems', *Compact heat exchanger 3rd edition*, Krieger publishing, Malabar, Florida, pp 121, (1984)